Pure appl. geophys. 161 (2004) 145–163
0033–4553/04/010145–19
DOI 10.1007/s00024-003-2432-y

Pure and Applied Geophysics

Nonlinear Time Series Analysis of Volcanic Tremor Events Recorded at Sangay Volcano, Ecuador

K. I. KONSTANTINOU[1] and C. H. LIN [1]

Abstract — The assumption that volcanic tremor may be generated by deterministic nonlinear source processes is now supported by a number of studies at different volcanoes worldwide that clearly demonstrate the low-dimensional nature of the phenomenon. We applied methods based on the theory of nonlinear dynamics to volcanic tremor events recorded at Sangay volcano, Ecuador in order to obtain more information regarding the physics of their source mechanism. The data were acquired during 21–26 April 1998 and were recorded using a sampling interval of 125 samples s^{-1} by two broadband seismometers installed near the active vent of the volcano. In a previous study JOHNSON and LEES (2000) classified the signals into three groups: (1) short duration (<1 min) impulses generated by degassing explosions at the vent; (2) extended degassing 'chugging' events with a duration 2–5 min containing well-defined integer overtones (1–5 Hz) and variable higher frequency content; (3) extended degassing events that contain significant energy above 5 Hz. We selected 12 events from groups 2 and 3 for our analysis that had a duration of at least 90 s and high signal-to-noise ratios. The phase space, which describes the evolution of the behavior of a nonlinear system, was reconstructed using the delay embedding theorem suggested by Takens. The delay time used for the reconstruction was chosen after examining the first zero crossing of the autocorrelation function and the first minimum of the Average Mutual Information (AMI) of the data. In most cases it was found that both methods yielded a delay time of 14–18 samples (0.112–0.144 s) for group 2 and 5 samples (0.04 s) for group 3 events. The sufficient embedding dimension was estimated using the false nearest neighbors method which had a value of 4 for events in group 2 and was in the range 5–7 for events in group 3. Based on these embedding parameters it was possible to calculate the correlation dimension of the resulting attractor, as well as the average divergence rate of nearby orbits given by the largest Lyapunov exponent. Events in group 2 exhibited lower values of both the correlation dimension (1.8–2.6) and largest Lyapunov exponent (0.013–0.022) in comparison with the events in group 3 where the values of these quantities were in the range 2.4–3.5 and 0.029–0.043, respectively. Theoretically, a nonlinear oscillation described by the equation $\ddot{x} + \beta\dot{x} + \gamma g(x) = f\cos\omega t$ can generate deterministic signals with characteristics similar to those observed in groups 2 and 3 as the values of the parameters β, γ, f, ω are drifting, causing instability of orbits in the phase space.

Key words: Volcanic tremor, degassing, chugging events, nonlinear dynamics, Sangay.

Introduction

The study of volcanic tremor poses two difficult problems that must be overcome in order for volcanoseismologists to obtain a better understanding of this

[1] Institute of Earth Sciences, Academia Sinica, P.O. Box 1-55, Nankang, Taipei, 115 Taiwan, R.O.C. E-mail: kostas@earth.sinica.edu.tw

phenomenon. The first problem is related to the restrictive assumptions that are usually made about the nature of the tremor source, requiring its description in terms of a linear oscillator that is set into resonance by a sudden sustained disturbance (e.g., FERRICK *et al*., 1982; CHOUET, 1985; LEET, 1988). The second problem concerns the selection of appropriate methods in order to investigate the properties of such signals, with spectral analysis being the method most commonly used. For a recent review of the methods and source modelling applied to volcanic tremor signals recorded at different volcanoes worldwide, the interested reader may refer to KONSTANTINOU and SCHLINDWEIN (2002).

The two problems mentioned above are interrelated and the suggestion put forward by some authors (SHAW, 1992; JULIAN, 1994) that a nonlinear process of some kind may be involved in tremor generation, requires one to reconsider which methods should be used in order to study it. Despite its usefulness for studying linear processes, spectral analysis can provide little insight into the physics of signals generated by nonlinear mechanisms. The main reason for this is the appearance of such signals in the frequency domain, which shows that they consist of a large number of frequencies resembling broadband random noise. The cause of this apparent randomness lies in the drifting of the parameters that control a nonlinear system, that may change its spectral character from periodic to completely broadband. This kind of behavior is defined as bifurcation (DRAZIN, 1994) and a series of repeated bifurcations will result in an aperiodic signal which is characterized as 'chaotic' (LI and YORK, 1975).

The methods based on the discipline of nonlinear dynamics utilize the notion of the phase or state space in order to describe how the behavior of a nonlinear system evolves as one or more of its parameters are bifurcating. This description is achieved by using an m-dimensional Euclidean space where m is proportional to the number of degrees of freedom present. The different states of the system define orbits that move around the phase space in such a way so as to accommodate three operations: (1) orbits should not intersect or overlap, since this would mean that the system revisits a previous state implying periodic and not chaotic behavior; (2) orbits should always move within a bounded region of the phase space due to dissipation of energy in the system; (3) orbits that are initially close may diverge exponentially from each other due to sensitivity to initial conditions. The geometrical object that is being formed as a result of these three operations has fractal properties and was called 'strange' attractor (RUELLE and TAKENS, 1971).

Nonlinear time series analysis uses all these concepts in order to devise practical methods for studying chaotic signals by reconstructing the phase space and extracting useful information about their driving mechanism. Even though such methods have been applied successfully to numerous nonlinear systems, their application to volcanic tremor time series is still elementary. CHOUET and SHAW (1991) were the first to investigate the phase space properties of volcanic tremor recorded at Pu'u O'o crater, Hawaii. Their study revealed a low value of the

Table 1

Summary of previously published fractal dimension values estimated from tremor time series recorded at different volcanoes

Volcano	Event type	D_F	Reference
Kilauea	Tremor	3.1–4.1	CHOUET and SHAW (1991)
Mt. Etna	Tremor	1.6	GODANO *et al.* (1996)
Stromboli	Low-frequency	2.68	GODANO and CAPUANO (1999)
Vulcano	Low-frequency	2.83–2.92	GODANO and CAPUANO (1999)
Vatnajökull	Tremor	3.5–4.0	KONSTANTINOU (2002)

fractal dimension D_F of the tremor attractor reaching an average value of 3.75. This was interpreted as an indication that tremor generation is not controlled by a stochastic process (where D_F should be infinite), therefore it can be described by only a few degrees of freedom. Subsequent studies of tremor recorded at Mt. Etna (GODANO *et al.*, 1996), low-frequency events from Stromboli and Vulcano islands (GODANO and CAPUANO, 1999) and tremor recorded during the 1996 Vatnajökull eruption in central Iceland (KONSTANTINOU, 2002) reported similar estimates of fractal dimensions (Table 1) confirming the low-dimensional nature of the phenomenon.

This paper describes the results obtained from the application of nonlinear time series analysis methods to tremor events recorded at Sangay volcano, Ecuador, in an effort to investigate whether the observed signals were generated by a nonlinear deterministic source. We chose to study this particular dataset for the following reasons: (1) the explosive activity and the seismic signals generated at Sangay share many similarities with those reported in many other volcanoes, such as Arenal in Costa Rica (BENOIT and MCNUTT, 1997), Karimsky in Russia (JOHNSON *et al.*, 1998) or Mt. Semeru in Indonesia (SCHLINDWEIN *et al.*, 1995), therefore our results may be relevant to these areas as well; (2) the duration of the tremor events is short enough so as to lower the computer time needed for the analysis and finely sampled so as to ensure that the tremor process is described adequately in the phase space. First, we give a brief overview of the available data and then we proceed to determine the optimum parameters for phase space reconstruction of the tremor attractor. Based on this reconstruction we try to quantify two important parameters that characterize a dynamic system: the number of the effective degrees of freedom (i.e., only those degrees of freedom relevant to the generation of tremor) given by the fractal dimension of the attractor and the degree of chaoticity (i.e., how substantially unpredictable is the behavior of our system) given by an estimation of the largest Lyapunov exponent. Finally, we discuss our results and compare them with those obtained by previous studies.

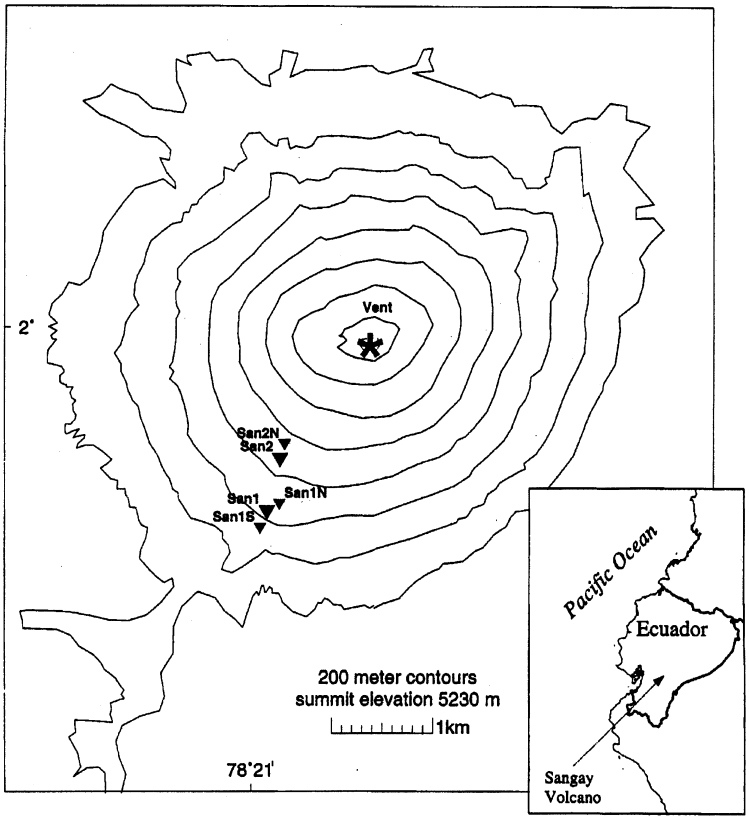

Figure 1
Map of Sangay and station locations. Stations SAN1 and SAN2 (large triangles) contained broadband seismometers and low-frequency microphones. Small triangles indicate the locations of single component short-period sensors. Inset map shows location of Sangay within South America (from JOHNSON and LEES, 2000).

Data Description and Selection

Sangay is the southernmost andesitic volcano of the Andean Northern Volcanic Zone and has been continuously active since 1628 (HALL, 1977). Field observations indicate that its activity consists mainly of summit vent explosions that eject ash and ballistics, but it may also consist of lava extrusions. This kind of activity is responsible for the accumulation of lava, debris and pyroclastic flows that created the 1800 m high Sangay edifice (MONZIER *et al.*, 1999). During 21–26 April 1998 two broadband three-component seismometers (Guralp CMG-40T) recording at a sampling interval of 125 samples s^{-1}, along with two electric condenser microphones were installed near the active summit vent (Fig. 1) in an effort to monitor the seismic and acoustic activity generated by the volcano. The spectral analysis of the seismic

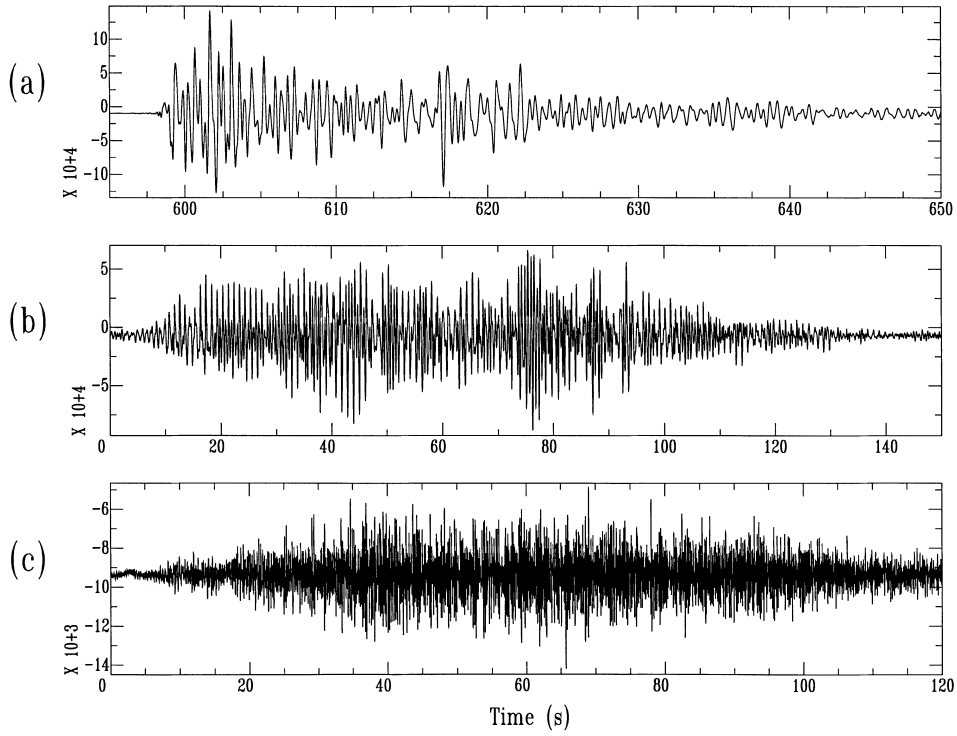

Figure 2
Example of vertical velocity waveforms of seismic signals recorded at station SAN2. (a) Short duration impulsive explosion event, (b) extended 'chugging' degassing event, (c) extended broadband degassing event. Note the different time scales.

and acoustic data as well as a classification of the seismic events recorded have been previously published by JOHNSON and LEES (2000), therefore only a summary of these aspects will be presented here.

JOHNSON and LEES (2000) grouped the seismic signals into three broad categories: (1) simple short duration (<1 min) impulses generated by degassing explosions at the vent (Fig. 2a); (2) extended degassing 'chugging' events of larger duration (2–5 min) containing well-defined integer overtones (1–5 Hz) and a variable higher frequency content, accompanied by sounds resembling those of a steam locomotive (Fig. 2b); (3) extended degassing events that contain significant energy above 5 Hz that may have resulted from the energetic jetting of material through the vent (Fig. 2c). The authors also noted the absence of background tremor for the whole of the observation period.

In the present study we have considered only the vertical component records from the two stations and tried to select suitable events from groups 2 and 3 for our analysis. The first criterion of suitability concerns the number of samples available in

Table 2

Sangay tremor events selected for analysis

Event #	Day	Station	Duration (s)	Samples	Type
1	112	SAN2	145	18,125	Broadband
2	112	SAN2	120	15,000	Broadband
3	112	SAN2	92	11,500	Broadband
4	112	SAN2	190	23,750	Broadband
5	111	SAN2	160	20,000	Chugging
6	112	SAN2	130	16,250	Chugging
7	112	SAN2	150	18,750	Chugging
8	114	SAN1	110	13,750	Chugging
9	115	SAN1	140	17,500	Chugging
10	115	SAN1	130	16,250	Chugging
11	116	SAN1	250	31,250	Chugging
12	116	SAN1	110	13,750	Chugging

each time series, since the methods for calculation of the fractal dimension or largest Lyapunov exponent need well-resolved phase space orbits in order to yield reliable results. The second criterion pertains to the level of noise present in the data, bearing in mind that noise levels larger than 2% may cause biased estimates of these quantities (KANTZ and SCHREIBER, 1996). Unfortunately, as it will be also mentioned in the next section, numerous events showed contamination with random noise, probably as a result of the weather conditions at the time of the experiment. The final dataset considered for this study consists of 12 broadband/chugging events with high signal-to-noise ratios and durations exceeding 90 seconds (Table 2).

Determination of Phase Space Reconstruction Parameters

Any time series generated by a nonlinear process can be considered as the projection on the real axis of a higher-dimensional geometrical object that describes the behavior of the system under study (KANTZ and SCHREIBER, 1996). The most common method used for phase space reconstruction of this object relies on the so-called Delay Embedding Theorem (TAKENS, 1981; SAUER *et al.*, 1991). This theorem states that a series of scalar measurements $s(t)$ (such as a seismogram) can be used in order to define the orbits describing the evolution of the states of the system in an m-dimensional Euclidean space. The orbits will then consist of points $\mathbf{x}$ with coordinates

$$\mathbf{x} = s(t), s(t+\tau), \ldots, s(t+(m-1)\tau) \tag{1}$$

where τ is referred to as the delay time and for a digitized time series is a multiple of the sampling interval used, while m is termed the embedding dimension. The

dimension m of the reconstructed phase space is considered as the sufficient dimension for recovering the object without distorting any of its topological properties, thus it may be different from the true dimension of the space where this object lies. Both the τ and m reconstruction parameters must be determined from the data.

Determination of the Delay Time

There are two possible ways to estimate the delay time required by the embedding theorem from an observed time series. The first is by calculating the autocorrelation function of the data and selecting as τ the time of its first zero-crossing. The reasoning behind this choice is that the time when the autocorrelation function reaches a zero value marks the point beyond where the $s(t+\tau)$ sample is completely decorrelated from $s(t)$. The second way involves the calculation from the data of a nonlinear autocorrelation function called Average Mutual Information (AMI) defined as (FRASER and SWINNEY, 1986)

$$I(\tau) = \sum_{ij} p_{ij}(\tau) \ln p_{ij}(\tau) - 2 \sum_{i} p_i(\tau) \ , \tag{2}$$

where p_i is the probability that the signal $s(t)$ takes a value inside the i-th bin of a histogram and p_{ij} is the probability that $s(t)$ is in bin i and $s(t+\tau)$ is in bin j. The first minimum in the AMI graph is considered as the most suitable choice for τ, since this is the time when $s(t+\tau)$ adds maximum information to the knowledge we have from $s(t)$.

Currently, there is no agreement among authors on which of the two methods should be used in order to determine the delay time. ABARBANEL (1996) objects to the use of the first zero-crossing of the autocorrelation function on the grounds that it takes into account only linear correlations of the data. On the other hand, KANTZ and SCHREIBER (1996) note that the estimation of τ using AMI is reliable only for two-dimensional embeddings. In most practical applications both methods are employed and it is either found that the estimated delay times are similar (FREDE and MAZZEGA, 1999) or that the two methods yield significantly different values of τ, in which case additional constraints may be needed (like the construction of two-dimensional phase portraits for different values of τ) in order to make a final decision (KONSTANTINOU, 2002).

For the Sangay tremor events we calculated both the autocorrelation function and AMI using timelags of 0–50 samples (0–0.4 s). The broadband events exhibited a fast first zero-crossing of the autocorrelation function at a timelag of five samples (0.04 s), in contrast to the chugging events that had a substantially slower decay to zero at timelags 14–18 samples (0.112–0.144 s) (Figs. 3a, b). For both groups of events AMI showed well-defined first minima (Figs. 3c, d) and in all cases the

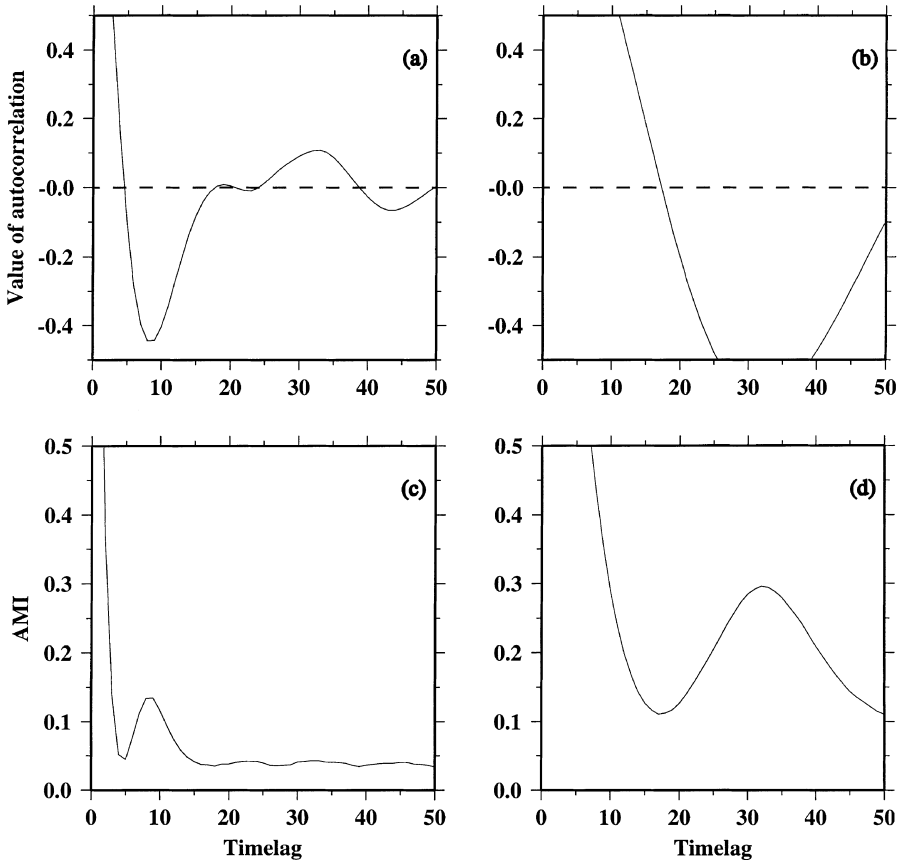

Figure 3
Example of selection of the delay time. Diagrams (a)–(c) show the autocorrelation function and Average Mutual Information (AMI) for a broadband event, while (b)–(d) show the same for a chugging event (see text for more details).

difference in the estimated delay time between the two methods was less than 1–2 samples (0.008–0.016 s).

Determination of the Embedding Dimension

The method used for the determination of the sufficient embedding dimension is based on the property of chaotic attractors in that their orbits should not intersect or overlap with each other. Such an intersection or overlap may result when the attractor is embedded in a dimension lower than the sufficient one stated by the delay embedding theorem. KENNEL *et al.* (1992) developed an algorithm that makes use of

this property in order to estimate the sufficient dimension for phase space reconstruction. Assuming that two points $\mathbf{x}^a$ and $\mathbf{x}^b$ are in proximity in the phase space, this is so either because the dynamic evolution of the orbits brought them close, or due to an overlap resulting from the projection of the attractor to a lower dimension. By comparing the Euclidean distance of the two points $|\mathbf{x}^a - \mathbf{x}^b|$ in two consecutive embedding dimensions d and $d+1$, it is possible to decipher which of the two possibilities is true. For embedding dimension m and delay time τ these distances are given by

$$R_d^2 = \sum_{m=0}^{d-1} [s^a(t+m\tau) - s^b(t+m\tau)]^2 \tag{3}$$

moving from dimension d to $d+1$ means that a new coordinate equal to $s(t+d\tau)$ is being added in each delay vector, so the Euclidean distance of the two points in dimension $d+1$ will be

$$R_{d+1}^2 = R_d^2(t) + |s^a(t+d\tau) - s^b(t+d\tau)|^2 \ . \tag{4}$$

The relative distance between the two points in dimensions d and $d+1$ will be the ratio

$$\sqrt{\frac{R_{d+1}^2 - R_d^2}{R_d^2}} = \frac{|s^a(t+d\tau) - s^b(t+d\tau)|}{R_d} \ . \tag{5}$$

If this distance ratio is greater than a predefined value s, then the points $\mathbf{x}^a$ and $\mathbf{x}^b$ are characterized as 'false' neighbors (being in the same neighborhood because of the projection and not because of the dynamics). An additional criterion for characterizing two points as false neighbors is that $R_{d+1} > \sigma/s$, where σ is the standard deviation of the data around its mean. Since σ can be considered as a representative measure of the size of the attractor, this criterion reflects the fact that if two points are false neighbors they will be stretched to the extremities of the attractor when they are separated from each other at dimension $d+1$. KENNEL *et al.* (1992) noted that a false nearest-neighbor algorithm that does not implement this second criterion will give an erroneous low embedding dimension even for high-dimensional stochastic processes. The procedure outlined above is repeated for all pairs of points at higher dimensions, until the percentage of the false neighbors becomes zero and then the attractor is said to be unfolded.

In order to apply the method to the tremor time series a suitable value for the distance ratio s had to be selected. ABARBANEL (1996) found that for many nonlinear systems this value approaches 15. This result was also confirmed in a study of tremor accompanying the 1996 Vatnajökull eruption in central Iceland, where s values in the range of 9–17 were found to produce stable false neighbors statistics (KONSTANTINOU, 2002). Therefore we used an s value of 15 and the delay times estimated in the previous section for calculating the percentage of false nearest-neighbours for each event.

Aside from determining the sufficient embedding dimension, the false nearest-neighbor method was also used as an indicator of the amount of noise in our data. As a stochastic process, noise should have infinite degrees of freedom and therefore it should show no tendency to unfold at any specific dimension. Thus we were able to eliminate events that showed a non-zero percentage of false neighbors in dimensions 1–10. For the rest of the events considered in this study the application of the method showed that for the broadband events the embedding dimension ranged 5–7 while for most of the chugging events the dimension was 4 (Fig. 4). Figures 5 and 6 show phase portraits of the reconstructed attractor for a broadband and a chugging event.

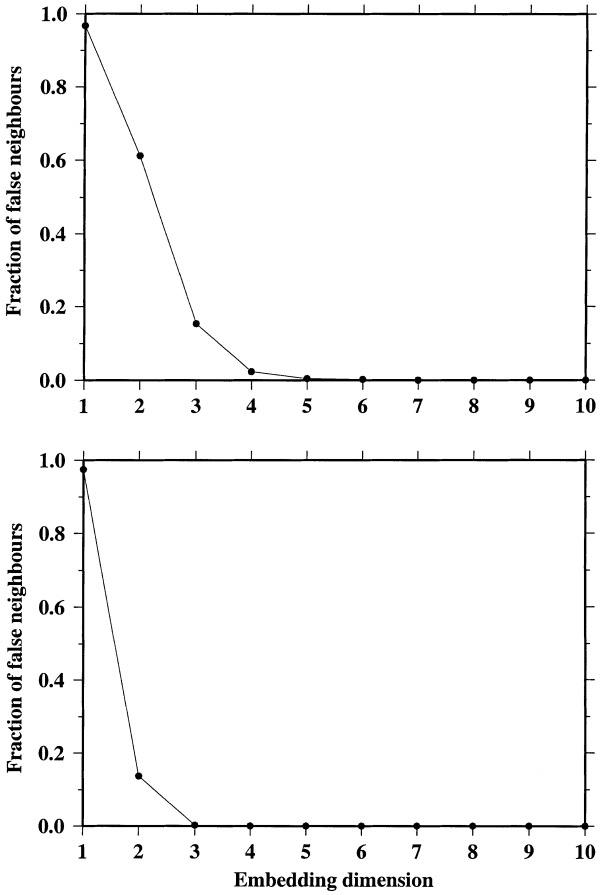

Figure 4
Top panel: Distribution of false nearest neighbors statistics for a broadband event in dimensions 1–10. The embedding dimension is 7, since in dimensions 5 and 6 there is still a very small percentage (0.004%–0.002%) of false neighbors. Lower panel: The same for a chugging event. The embedding dimension is 4, since in dimension 3 there is still a percentage (0.001%) of false neighbors.

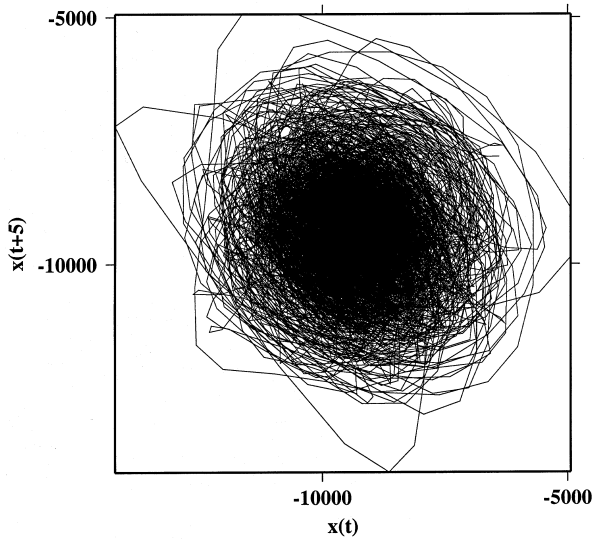

Figure 5
Two-dimensional phase portrait of a broadband event reconstructed for $\tau = 5$.

Estimation of Correlation Dimension

As mentioned earlier, the attractor resulting from the embedding procedure is a fractal object and the estimation of its dimension forms a part of every successful nonlinear time series analysis. The importance of the fractal dimension stems mainly from two reasons: (1) it gives a measure of the effective degrees of freedom that are present in the physical system under study; (2) it is a quantity that does not vary under smooth transformations of the coordinate system (i.e., an 'invariant measure'). Even though there exists a number of definitions for the dimension of a fractal object (Box-counting dimension, Information dimension, etc.), the correlation dimension definition suggested by GRASSBERGER and PROCACCIA (1983) was found to be the most efficient for practical applications. For an N number of points $\mathbf{x}_n$ resulting from the embedding and for distance values r, the correlation sum definition as modified by THEILER (1990) is

$$C(r) = \frac{2}{(N - n_{\min})(N - n_{\min} - 1)} \sum_{i=1}^{N} \sum_{j=i+n_{\min}}^{N} \Theta(r - |\mathbf{x}_i - \mathbf{x}_j|) \tag{6}$$

where Θ is the Heaviside step function, with $\Theta(x) = 0$ if $x \leq 0$ and $\Theta(x) = 1$ for $x > 0$. The quantity $n_{\min}$ (also known as 'Theiler window') represents the number of points that must be excluded from the calculation of $C(r)$ because they are temporally correlated. The consequence of not including this correction in the calculation of the correlation sum is that the correlation dimension obtained

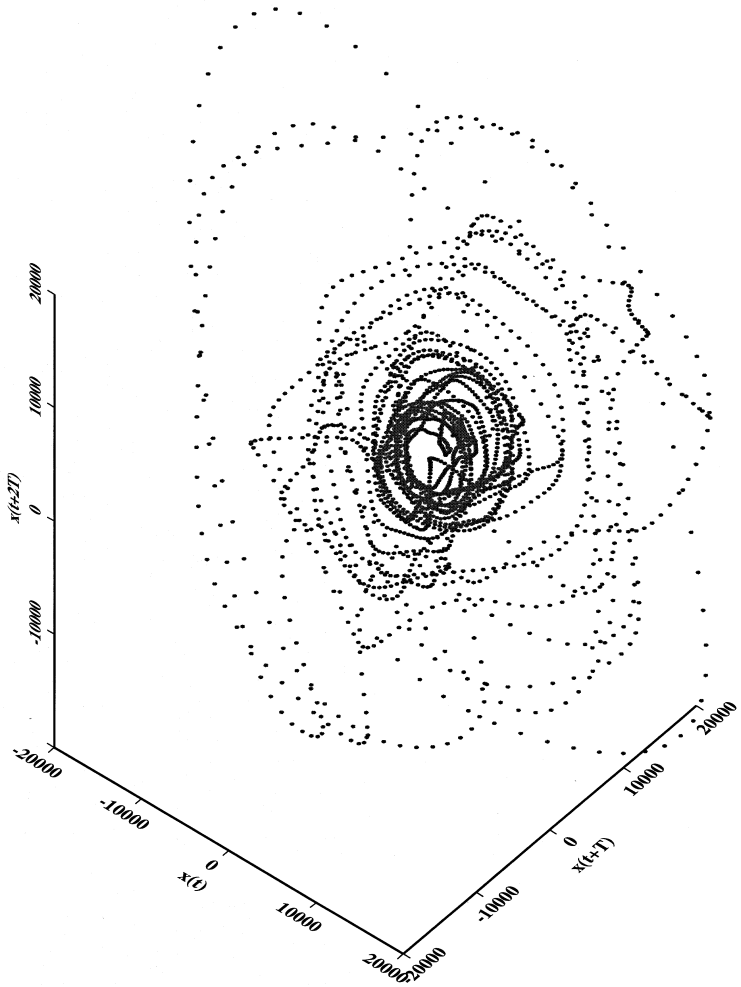

Figure 6
Three-dimensional phase portrait of a chugging event reconstructed for $\tau = 14$. For clarity only the first 22 s of the signal have been embedded. Since the percentage of false neighbors in dimension 3 is very small for all chugging events, the attractor shown is almost unfolded. The structure near the center of the plot represents the first harmonic oscillation cycles which later become unstable, giving rise to chaotic orbits that move within a larger portion of the phase space.

subsequently would be erroneously low (THEILER, 1990). In the limit of an infinite amount of data and for vanishingly small r, the correlation sum should scale like a power law $C(r) \sim r^D$ and the correlation dimension is then defined as

$$d(N,r) = \frac{\ln C(r,N)}{\ln r} \quad . \tag{7}$$

We calculated the correlation sum for our dataset using the delay times determined in the previous section and for embedding dimensions 1–10. The minimum value of r was equal to the maximum data interval divided by 1000, while we chose a value for the Theiler window, recommended by KANTZ and SCHREIBER (1996), of 500 (the data portion omitted in time units is $t_{\min} = n_{\min}\Delta t = 500 \times 0.008 = 4$ s, with Δt being the sampling interval).

The next step was to calculate $d(N, r)$ and plot it against r, so that scaling regions in the plot could be identified by visual inspection (Fig. 7). In theory, it is expected that for a low-dimensional chaotic sytem, each curve representing an embedding dimension equal or higher to the sufficient one should saturate at a particular value

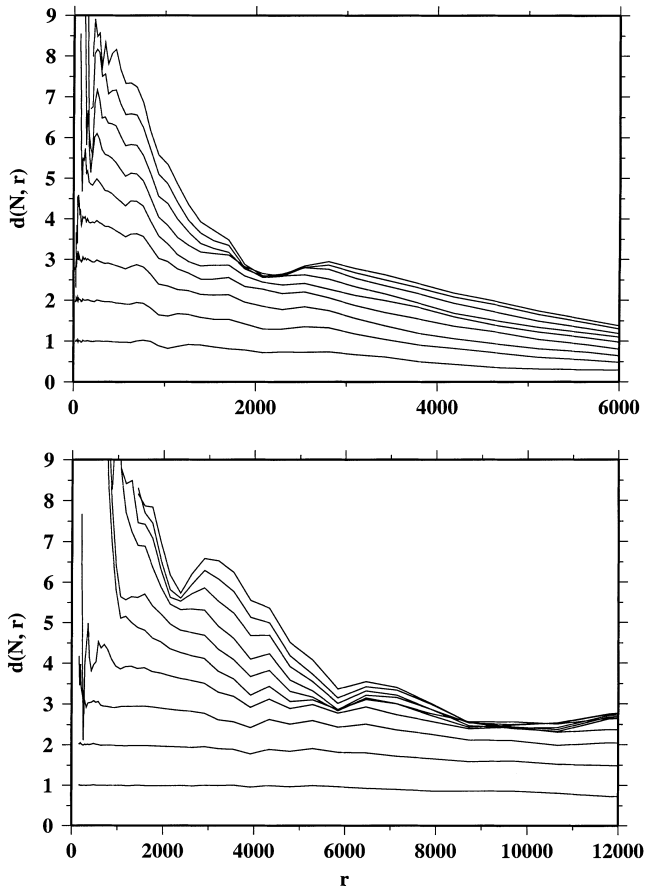

Figure 7
Top panel: Slope of the correlation sum $d(N, r)$ versus r for a broadband event showing a scaling region around $r = 2000$. The saturation effect is clear after dimension 5. Lower panel: The same for a chugging event showing a scaling region for $r = 9000$–11000. Here the saturation effect is clear after dimension 3.

of $d(N, r)$. This value may *then* be interpreted as the correlation dimension v of the system. Broadband events exhibited correlation dimension values in the range 2.4–3.5, while for all chugging events the values were lower (1.8–2.6) except from event 11 that showed no clear scaling region. All events excepting 1 and 8 yielded dimension estimates not higher than the maximum implied by the embedding theorem $v < m/2$, which shows that the false nearest neighbors method gives in most cases a reliable estimate of the embedding dimension.

An issue that is raised in all studies that attempt to estimate the correlation dimension from a time series, concerns the minimum number of points needed for this estimation to be meaningful. RUELLE (1990) showed that a necessary condition for a reliable estimation of v is that $v \leq 2 \log N$ where N is the number of samples used in the calculation. It can be easily verified by substituting the appropriate N values for each event that the quantity $2 \log N$ is in the range 8.121–8.602 and is always larger than the estimated correlation dimensions.

However, URQUIZÚ and CORREIG (1998) reported that subsequently Ruelle (unpublished work) recognized that this condition, even though it is necessary, may not be sufficient. A supplementary condition is that the best number of data points is reached when each axis of the embedding phase space contains a minimum of 10 independent values, so that in total the minimum number of samples should be 10^m with m being the embedding dimension. This means that for the chugging events where $m = 4$ the minimum number of points is 10^4 and since the lengths of the time series is in the range of 13,750–31,250 samples, this condition is also satisfied. For the broadband events it is obvious that the available samples (11,500–23,750) are far fewer than the large minimum numbers (10^5, 10^6, 10^7) implied by the sufficient condition for $m = 5, 6, 7$. We accept therefore that these dimension estimates are characterized by a degree of uncertainty.

Estimation of the Largest Lyapunov Exponent

Exponential divergence of nearby orbits in phase space is recognised as the hallmark of chaotic behavior (DRAZIN, 1994). If we again take two points in the phase space $\mathbf{x}_{n_1}$ and $\mathbf{x}_{n_2}$ and indicate their distance as $|\mathbf{x}_{n_1} - \mathbf{x}_{n_2}| = \delta_0$ then after time t it is expected that the new distance δ will be equal to $\delta = \delta_0 e^{\lambda t}$, where $\lambda > 0$ is called the Lyapunov exponent. For a low-dimensional deterministic process the Lyapunov exponent should be a positive finite number, for a linear process it should be zero and for a stochastic process it should be infinite. In general, for an m-dimensional phase space the rate of expansion or contraction of orbits is described for each direction by a Lyapunov exponent, resulting in m different Lyapunov exponents of which some are zero or negative. However, the main interest is focused on the largest of these exponents since it can be calculated relatively easy and it yields evidence for the presence of deterministic chaos in the observed data.

ROSENSTEIN *et al.* (1993) proposed a method to calculate the largest Lyapunov exponent from an observed times series. After reconstructing the phase space using suitable values for τ and m, a point $\mathbf{x}_{n_0}$ is chosen and all neighbor points $\mathbf{x}_n$ closer than a distance r are found and their average distance from that point is calculated. This is repeated for N number of points along the orbit so as to calculate an average quantity S known as the stretching factor

$$S = \frac{1}{N}\sum_{n_0=1}^{N}\left(\ln\frac{1}{|\mathcal{U}_{x_{n_0}}|}\sum|\mathbf{x}_{n_0}-\mathbf{x}_n|\right) \ , \tag{8}$$

where $|\mathcal{U}_{x_{n_0}}|$ is the number of neighbors found around point $\mathbf{x}_{n_0}$. A plot of the stretching factor S versus the number of points N (or time $t = N\Delta t$) will yield a curve with a linear increase at the beginning, followed by an almost flat region. The first part of this curve represents the exponential increase of S as more points from the orbit are included, while the flat region signifies the saturation effect of exponential divergence due to the finite size of the attractor. A least-squares line fit for the slope of the linear part of the curve would then yield an estimation of the largest Lyapunov exponent. ROSENSTEIN *et al.* (1993) used known chaotic systems in order to test their algorithm and found that the largest Lyapunov exponents they obtained approximated $\pm 10\%$ of the correct value when the noise level, embedding parameters and data length were varied within reasonable bounds.

We applied the method described above to both the broadband and the chugging events, using the same embedding parameters as before. The value of r was taken as the data interval divided by 1000, and again, in order to avoid temporal correlations we used a Theiler window of 500. The curves for both groups of events showed the expected linear increase/flat regions (Fig. 8) with some fluctuations superimposed on the linear part of the curve, which for Event 1 were quite large and therefore no attempt to fit a straight line was made. These fluctuations can be explained based on the fact that the stretching factor is just an average of the local stretching or shrinking rates in the attractor, therefore these different rates may not always be smoothed by the averaging process of the algorithm (KANTZ and SCHREIBER, 1996). The slope values corresponding to the largest Lyapunov exponent were obtained after the least-squares line fit for the rest of the events. Table 3 summarizes the estimated embedding parameters, correlation dimension values and largest Lyapunov exponents for the events under study.

Discussion

Chaotic signals are characterized by at least one positive Lyapunov exponent and a low-dimensional fractal attractor in the phase space. These characteristics have been found in both broadband and chugging tremor signals recorded at Sangay, and

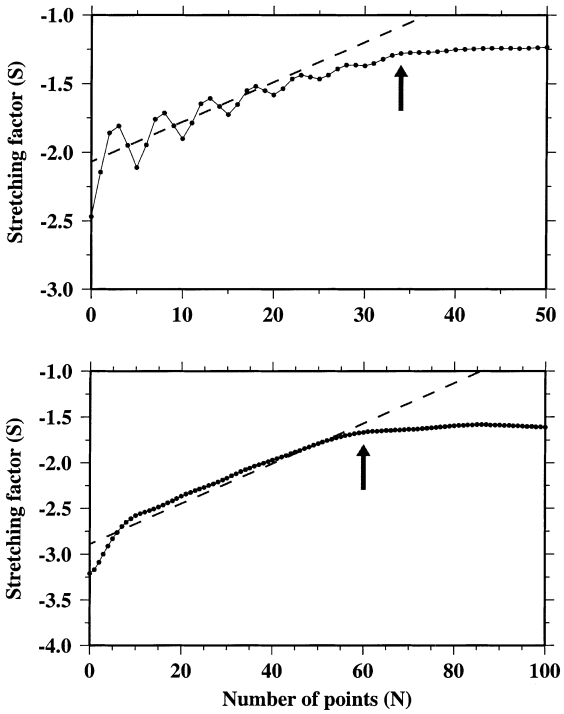

Figure 8

Top panel: Estimation of the largest Lyapunov exponent using the method of ROSENSTEIN *et al.* (1993) for a broadband event. The portion of the curve used for the least-squares line fit starts from the beginning until the saturation point shown by the arrow. The dashed line represents the resulting least-squares line fit. Lower panel: The same for a chugging event.

Table 3

Summary of the estimated delay time (τ), embedding dimension m, correlation dimension v and largest Lyapunov exponent (λ) for each of the 12 tremor events under study

Event #	τ	m	v	λ
1	15	5	2.7	–
2	5	7	3.5	0.029
3	5	5	2.5	0.041
4	5	6	2.4	0.043
5	18	4	1.2	0.013
6	14	4	1.7	0.021
7	17	4	1.9	0.016
8	14	4	2.6	0.020
9	15	4	1.8	0.018
10	14	4	1.8	0.022
11	15	5	–	0.012
12	16	4	1.8	0.022

at least their fractal dimension values (we are not aware of any other study in which where an estimate of the largest Lyapunov exponent for tremor data is given) range equally with those published by other authors (Table 1). This result is added to the growing body of observational evidence that suggests that volcanic tremor sources excited by possibly different physical mechanisms (e.g., magma flow in great depths or gas exsolution in shallow depths), may generate low-dimensional signals with similar phase space properties.

Another interesting result stemming from our analysis regards the phase space properties of the broadband and chugging events. A comparison of the values of the correlation dimension and largest Lyapunov exponent (Table 3) of the two groups shows that the broadband events possess both larger correlation dimensions and Lyapunov exponent values than the chugging events. On the other hand, chugging events that contain a higher frequency content show higher dimensions and Lyapunov exponent values than those events in which the integer overtones seem to dominate.

Based on these observations it is only possible to derive a qualitative model of the source that may be generating the observed signals. The low values of the correlation dimension (1.8–3.5) suggest that a second-order nonlinear differential equation may be enough to describe the Sangay tremor source. A large number of forced nonlinear oscillators described by the general equation

$$\ddot{x} + \beta\dot{x} + \gamma g(x) = f \cos \omega t \ , \tag{9}$$

where β is the damping coefficient, $g(x)$ contains the nonlinear terms and $f \cos \omega t$ is the forcing term, may be good candidates for such a modelling.

It can be shown theoretically (JORDAN and SMITH, 1987) that solutions of this equation with a frequency which is an integer multiple of the forcing frequency ω are possible in the case of weak nonlinearity ($|\gamma| < 1$) and may correspond to the harmonics observed in the chugging events. Furthermore, these solutions can become unstable in the phase space through a series of repeated bifurcations as the parameters $(\beta, \gamma, f, \omega)$ start drifting. This would gradually change the spectral character of the signal to broadband and also increase the Lyapunov exponent from an initial zero value (for a purely harmonic behavior) to a positive number. This transition therefore may explain the variable higher frequency content, largest Lyapunov exponents and correlation dimensions observed in the recorded tremor events. Similar analogue modelling has been suggested by GODANO and CAPUANO (1999) for low-frequency earthquakes recorded at Stromboli and Vulcano volcanoes in Italy. The authors noted the similarity of the time domain and phase space characteristics of the observed data and the solutions of the nonlinear oscillator described by equation (9) with $g(x) = -\frac{1}{2}(1 - x^2)$.

However, this kind of modelling leaves open a number of important issues. First, the exact physical mechanism causing these nonlinear oscillations and the physical meaning of the terms γ and $g(x)$ are uncertain. JOHNSON and LEES (2000) reported, based on visual observations, the presence of rubble and rising viscous lava at the top

part of the active vent. Assuming that there is unsteady gas flow inside the vent, they suggest that this material may be acting as a kind of valve in a pressurized system, regulating the escape of gas into the atmosphere in an oscillatory manner that results in the generation of the observed signals. Second, the description of such a behavior in terms of a system of coupled nonlinear differential equations will probably introduce more numerous degrees of freedom than those implied by our analysis. Therefore a means of compressing this number to a minimum, while maintaining the same dynamics with the observations, should be found. Hopefully both of these issues will be resolved in future theoretical modelling efforts.

Even though the results of the application of nonlinear time series analysis methods to volcanic tremor events can tell us what kind of oscillatory behavior we are dealing with (linear/nonlinear, stochastic/deterministic) and how many degrees of freedom are involved, they cannot provide a clue as to what the physical mechanism of this oscillation is. Other methods, that can extract information concerning the physical properties and geometrical configuration of the rock-fluid system from seismic and acoustic data combined with visual observations, are needed in order to accomplish this task. Future volcano monitoring efforts should, therefore, rely on a multidisciplinary approach when trying to study the nature of volcanic tremor sources.

Acknowledgements

This research was supported by the Institute of Earth Sciences, Academia Sinica through a postdoctoral research fellowship awarded to the first author. Mike Hagerty and an anonymous reviewer read the manuscript and contributed many helpful comments. The TISEAN software package (HEGGER *et al.*, 1999) was used for the nonlinear time series analysis of the data. Jeff Johnson kindly provided us with the original figure of the Sangay station deployment.

REFERENCES

ABARBANEL, H. D. I., *Analysis of Observed Chaotic Data* (Springer, New York, 1996).

BENOIT, J. and MCNUTT, S. R. (1997), *New Constraints on the Source Processes of Volcanic Tremor at Arenal Volcano, Costa Rica, Using Broadband Seismic data*, Geophys. Res. Lett. *24*, 449–452.

CHOUET, B. A. (1985), *Excitation of a Buried Magmatic Pipe: A Seismic Source Model for Volcanic Tremor*, J. Geophys. Res. *90*, 1881–1893.

CHOUET, B. A. and SHAW, H. R. (1991), *Fractal Properties of Tremor and Gas-piston Events Observed at Kilauea Volcano, Hawaii*, J. Geophys. Res. *96*, 10177–10189.

DRAZIN, P. G., *Nonlinear Systems* (Cambridge University Press, New York, 1994).

FERRICK, M. G., QAMAR, A., and ST. LAWRENCE, W. F. (1982), *Source Mechanism of Volcanic Tremor*, J. Geophys. Res. *87*, 8675–8683.

FRASER, A. M. and SWINNEY, H. L. (1986), *Independent Coordinates for Strange Attractors from Mutual Information*, Phys. Rev. A *87*, 1134–1140.

FREDE, V. and MAZZEGA, P. (1999), *Detectibility of Deterministic Nonlinear Processes in Earth Rotation Time Series I. Embedding*, Geophys. J. Int. *137*, 551–564.

GODANO, C., CARDACI, C., and PRIVITERA, E. (1996), *Intermittent Behaviour of Volcanic Tremor at Mt. Etna*, Pure Appl. Geophys. *147*, 729–744.

GODANO, C. and CAPUANO, P. (1999), *Source Characterisation of Low Frequency Events at Stromboli and Vulcano Islands (Isole Eolie Italy)*, J. Seismol. *3*, 393–408.

GRASSBERGER, P. and PROCACCIA, I. (1983), *Characterisation of Strange Attractors*, Phys. Rev. Lett. *50*, 346–349.

HALL, M. L., *Volcanism in Ecuador*, Institute of Geography and History, Quito (in Spanish), 1977.

HEGGER, R., KANTZ, H., and SCHREIBER, T. (1999), *Practical Implementation of Nonlinear Time Series Methods: The TISEAN Package*, CHAOS *9*, 413.

JOHNSON, J. B., LEES, J. M., and GORDEEV, E. I. (1998), *Degassing Explosions at Karimsky Volcano, Kamtchaka*, Geophys. Res. Lett. *25*, 3999–4002.

JOHNSON, J. B. and LEES, J. M. (2000), *Plugs and Chugs—Seismic and Acoustic Observations of Degassing Explosions at Karimsky, Russia and Sangay, Ecuador*, J. Volc. Geotherm. Res. *101*, 67–82.

JORDAN, D. W. and SMITH, P., *Nonlinear Ordinary Differential Equations* (Oxford University Press, Clarendon, 1987).

JULIAN, B. R. (1994), *Volcanic Tremor: Nonlinear Excitation by Fluid Flow*, J. Geophys. Res. *99*, 11859–11877.

KANTZ, H. and SCHREIBER, T., *Nonlinear Time Series Analysis* (Cambridge University Press, Cambridge, 1996).

KENNEL, M. B., BROWN, R., and ABARBANEL, H. D. I. (1992), *Determining Embedding Dimension for Phase Space Reconstruction Using a Geometrical Construction*, Phys. Rev. A *45*, 3403–3411.

KONSTANTINOU, K. I. (2002), *Deterministic Nonlinear Source Processes of Volcanic Tremor Signals Accompanying the 1996 Vatnajökull Eruption, Central Iceland*, Geophys. J. Int. *148*, 663–675.

KONSTANTINOU, K. I. and SCHLINDWEIN, V. (2002), *Nature, Wavefield Properties and Source Mechanism of Volcanic Tremor: A Review*, J. Volc. Geotherm. Res., in press.

LEET, R. C. (1988), *Saturated and Subcooled Hydrothermal Boiling in Groundwater Flow Channels as a Source of Harmonic Tremor*, J. Geophys. Res. *93*, 4835–4849.

LI, T. Y. and YORK, J. A. (1975), *Period Three Implies Chaos*, Am. Math. Mon. *82*, 985–982.

MONZIER, M., ROBIN, C., SAMANIEGO, P., HALL, M. L., MOTHES, P., ARNAUD, N., and COTTEN, J. (1999), *Sangay Volcano (Ecuador): Structural Development and Petrology*, J. Volc. Geotherm. Res. *90*, 49–79.

ROSENSTEIN, M. T., COLLINS, J. J., and DELUCA, C. J. (1993), *A Practical Method for the Calculating Largest Lyapunov Exponents from Small Datasets*, Physica D *65*, 117–134.

RUELLE, D. (1990), *Deterministic Chaos: The Science and the Fiction*, Proc. Roy. Soc. London A*427*, 241–248.

RUELLE, D. and TAKENS, F. (1971), *On the Nature of Turbulence*, Commun. Math. Phys. *20*, 167–192.

SAUER, T., YORK, J. A., and CASDAGLI, M. (1991), *Embedology*, J. Stat. Phys. *65*, 579.

SCHLINDWEIN, V., WASSERMAN, J., and SCHERBAUM, F. (1995), *Spectral Analysis of Harmonic Tremor Signals from Mt. Semeru, Indonesia*, Geophys. Res. Lett. *22*, 1685–1688.

SHAW, H. R. (1992), *Nonlinear Dynamics and Magmatic Periodicity; Fractal Intermittency and Chaotic Crises*, Int. Geol. Congr., 510.

TAKENS, F., *Detecting Strange Attractors in Turbulence*, Lecture notes in Math., (Springer, New York, 1981).

THEILER, J. (1990), *Estimating Fractal Dimension*, J. Opt. Soc. Am. *7*, 1055–1073.

URQUIZÚ, M. and CORREIG, A. M. (1998), *Analysis of Seismic Dynamical Systems*, J. Seismol. *2*, 159–171.

(Received May 9, 2002, accepted October 21, 2002)